Accounting for Quasi-Static Coupling in Nonlinear Dynamic Reduced-Order Models

Evangelia Nicolaidou*
Department of Mechanical Engineering
University of Bristol
Bristol, BS8 1TR
United Kingdom
e-mail: e.nicolaidou@bristol.ac.uk

Venkata R. Melanthuru
Department of Mechanical Engineering
University of Bristol
Bristol, BS8 1TR
United Kingdom

Thomas L. Hill
Department of Mechanical Engineering
University of Bristol
Bristol, BS8 1TR
United Kingdom

Simon A. Neild
Department of Mechanical Engineering
University of Bristol
Bristol, BS8 1TR
United Kingdom

Engineering structures are often designed using detailed Finite Element (FE) models. Although these models can capture nonlinear effects, performing nonlinear dynamic analysis using FE models is often prohibitively computationally expensive. Nonlinear reduced-order modelling provides a means of capturing the principal dynamics of an FE model in a smaller, computationally cheaper Reduced-Order Model (ROM). One challenge in formulating nonlinear ROMs is the strong coupling between low- and high-frequency modes, a feature we term quasi-static coupling. *An example of this is the coupling between bending and axial modes of beams. Some methods for formulating ROMs require that these high-frequency modes are included in the ROM, thus increasing its size and adding computational expense. Other methods can implicitly capture the effects of the high-frequency modes within the retained low-frequency modes; however, the resulting ROMs are normally sensitive to the scaling used to calibrate them, which may introduce errors. In this paper, quasi-static coupling is first investigated using a simple oscillator with nonlinearities up to the cubic order. Reduced-order models typically include quadratic and cubic nonlinear terms, however here it is demonstrated mathematically that the ROM describing the oscillator requires higher-order nonlinear terms to capture the modal coupling. Novel ROMs, with high-order nonlinear terms, are then shown to be more accurate, and significantly more robust to scaling, than standard ROMs developed using existing approaches. The robustness of these novel ROMs is further demonstrated using a clamped-clamped beam, modeled using commercial FE software.*

1 Introduction

Many modern engineering structures are required to operate in extreme environments, or are designed with operating envelopes that go beyond the regions where linear behavior can be assumed. For example, the skin panels of hypersonic aircraft experience extreme thermal, aerodynamic and

*Corresponding author.

acoustic loads [1, 2]; similarly, highly flexible aircraft have great potential for improved aerodynamic efficiency, but the large deflections they exhibit lead to highly nonlinear behavior [3]. These extreme structures and environments require nonlinear dynamic behavior to be considered at many stages of the design process.

Numerous tools and techniques may be employed for analysing nonlinear dynamic behavior. For example, analytical approaches – such as the harmonic balance, multiple scales and normal form methods [4–6] – allow the responses of nonlinear systems to be analysed in detail and approximate solutions to be found explicitly [7]. Alternatively, numerical continuation techniques allow nonlinear responses to be computed accurately and efficiently without the need for analytical treatment [8, 9]. These analytical and numerical techniques are typically applied to the nonlinear equations of motion describing a structure; however, in engineering disciplines, Finite Element (FE) models are often used, rather than explicit equations of motion, to model structures. Although FE analysis allows models of highly complex structures to be developed efficiently, using the models directly to predict nonlinear dynamic behavior is often extremely computationally expensive [10]. Nonlinear reduced-order modelling provides a means of capturing the properties of a structure that govern the nonlinear dynamic behavior of interest. These Reduced-Order Models (ROMs) take the form of low-order systems of nonlinear equations of motion which may be interrogated using the aforementioned analytical and numerical tools, allowing for detailed, and computationally efficient, analysis of complex structures.

As described in the review by Mignolet *et al.* [11], techniques for nonlinear model-order reduction may be separated into two main categories: *direct*, where the nonlinear equations of motion of the full-order system are known and accessible; and *indirect*, where the equations of motion are inaccessible or are not explicitly formulated. The focus of the current paper is on indirect methods, which may be applied to any commercial FE software that allows nonlinear static solutions to be computed, such as Abaqus [12].

The two main indirect methods for nonlinear reduced-order modelling are the *enforced displacement* and *applied loads* methods. These two approaches have the same objective: to determine the relationship between the modal forces (i.e. forces in the shapes of the linear modes) and modal displacements, and use this relationship to calibrate an assumed nonlinear stiffness model. In both cases, it is therefore assumed that the dynamics of interest may be captured by a limited number of linear modal coordinates, which form the ROM basis. The enforced displacement method, which was first developed by Muravyov and Rizzi [13, 14], determines the modal force-displacement relationship by applying a set of modal displacements to the FE model and measuring the forces required to achieve these displacements. The applied loads procedure, first introduced by Segalman *et al.* [15, 16], instead applies a series of loads to the FE model and measures the resulting displacements.

Whilst the applied loads and enforced displacement approaches may seem equivalent, a number of differences have been noted. For example, the enforced displacement method is relatively insensitive to the amplitude of the displacements used to calibrate the model [13]. However, this method does not capture the effects of the coupling between membrane and axial modes and, as such, typically requires multiple axial modes to be explicitly included in the ROM basis [17]. On the other hand, the applied loads procedure is able to capture the membrane stretching effect implicitly; however, the resulting ROM is often sensitive to the amplitudes of the modal forces used for calibrating it [2]. As such, the ROM may be *tuned* using the forcing amplitudes. The mechanism that governs this coupling has recently been explored by Tartaruga *et al.* [18].

This paper investigates the mechanism that underpins *quasi-static coupling* between low- and high-frequency modes of nonlinear systems. Quasi-static coupling describes coupling between modes of a system that causes the behavior of one mode to be dictated by another. Membrane stretching is an example of quasi-static coupling – i.e. the axial modes are assumed to be a function of the membrane modes – but a more general term is employed here to account for similar effects in systems without *membrane-like* features, such as the simple oscillator considered as a motivating example in §2. The effect of quasi-static coupling is investigated in detail using the applied loads procedure, and it is demonstrated that a ROM that is insensitive to the forcing amplitude may exist. Specifically, it is demonstrated that this coupling causes the order of the nonlinearity of the ROM to increase – i.e. even though the full-order system contains only cubic nonlinearities, the ROM must include nonlinearities of order higher than cubic in order to accurately capture its response. This is in contrast with existing approaches, where the nonlinearity in the ROMs is limited to the cubic order [11]. It is demonstrated that using a higher-order of nonlinearity in the ROM not only leads to a more robust parametric fitting procedure using the applied loads method, but that the resulting ROMs can be significantly more accurate.

The paper is structured as follows: §2 introduces a simple, 2-DoF oscillator which exhibits a quasi-static coupling between its two modes – this is used as a motivating example to demonstrate the effect of including higher orders of nonlinearity in the ROMs. This system is again considered in §3 and, after formalising the quasi-static coupling, it is used to demonstrate that an *exact* ROM – i.e. a ROM that is invariant to the amplitude of the static loads – does exist, but that it requires a high order of nonlinearity in the ROM. The backbone curves (or, equivalently, the nonlinear normal modes) are used to compare the accuracy of the different ROMs. Finally, in §4, the approach is demonstrated using a clamped-clamped beam, modeled in the commercial FE software Abaqus. This further highlights the robustness that is gained from including higher orders of nonlinearity in ROMs of more complex structures, thus eliminating the need for fine-tuning and extending the applicability of the resulting ROM to a wider range of operating conditions.

2 A simple, strongly coupled oscillator

Quasi-static coupling describes when the linear modes of a system are coupled such that the motion of one mode may be expressed as a function of another. For example, as shown in Fig. 1, the tip of a thin, cantilever beam will move towards the root of the beam when bending with a large deflection. This may be viewed as an axial displacement of the beam; however, this axial motion is a function of vertical deflection, rather than an independent behavior (provided the axial stiffness is much greater than the vertical stiffness). A beam is considered in §4, however, first, a conceptually simple system is used to demonstrate the quasi-static coupling effects and examine their influence on the process of reduced-order modelling.

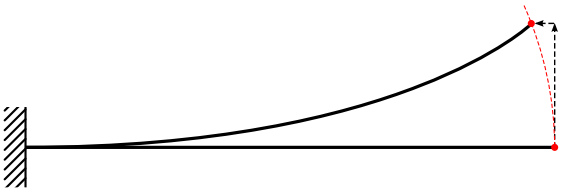

Fig. 1. A schematic depicting the axial motion of the tip of a cantilever beam undergoing a large deflection. The dashed-red line shows the path of the tip of the beam.

2.1 A simple two-degree-of-freedom oscillator

Figure 2 shows a schematic of a simple, one-mass oscillator that is free to move in the horizontal (x) and vertical (y) directions. It is constrained by two springs with lengths $\ell_1 = 0.1\,\mathrm{m}$ and $\ell_2 = 0.1\,\mathrm{m}$ respectively, and linear stiffness parameters $k_1 = 10\,\mathrm{N\,m^{-1}}$, and $k_2 = 1000\,\mathrm{N\,m^{-1}}$, respectively. When $x = y = 0$, these springs are orthogonal and in equilibrium. It is assumed that this is a point mass ($m = 0.1\,\mathrm{kg}$), and hence does not rotate; as a result, this system has two degrees-of-freedom. This structure has previously been considered by Touzé et al. [19], and used to demonstrate a reduced-order modelling procedure in [20].

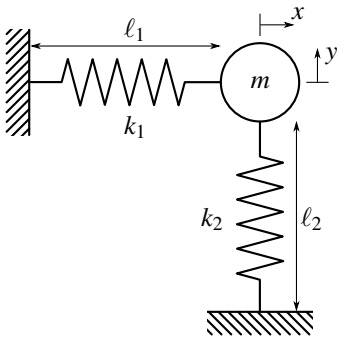

Fig. 2. A schematic diagram of a two-degree-of-freedom, single-mass oscillator, used as a simple motivating example.

As the two springs are orthogonal and have no pretension, the first linear mode of the system is captured by a purely horizontal (x-direction) motion, whilst the motion of the second mode is purely vertical (y-direction). As $k_2 \gg k_1$, the second linear natural frequency is considerably greater than the first. Additionally, if the mass is deflected horizontally (i.e. in the first mode), the strong coupling between the modes (due to the geometry of the system) will cause a deflection in the vertical direction (i.e. the second mode). For small dynamic displacements in the first mode, the mass will follow an *arced* path – as shown in Fig. 3[1]. This response clearly shows a displacement in the vertical direction; however, rather than being an independent degree-of-freedom, the vertical displacement may be considered to be a function of the horizontal displacement, i.e. $y = f(x)$. This is analogous to the cantilever beam shown in Fig. 1, which also exhibits two strongly coupled modes with a large difference in their natural frequencies (i.e. the bending and axial modes). Note that in the extreme case of $k_2 \to \infty$, this system will represent a pendulum constrained by a spring – a system with only one degree-of-freedom (DoF), and which exhibits a similar response to that shown in Fig. 3.

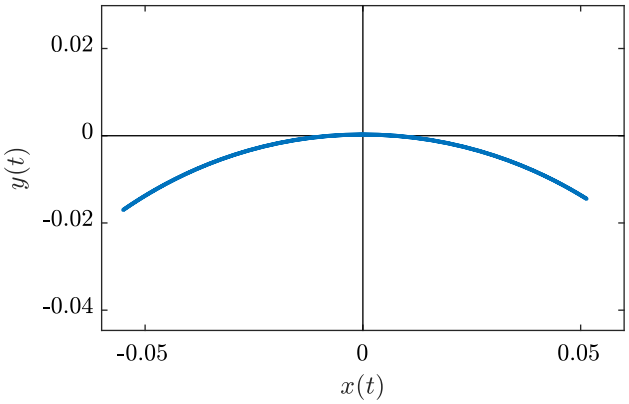

Fig. 3. A free, periodic response of the two-degree-of-freedom oscillator. This is shown in the projection of the horizontal displacement, x, against the vertical displacement, y, parameterised in time.

The equations of motion of the 2-DoF system in Fig. 2 are written

$$m\ddot{x} + F_x(x,y) = 0\,, \tag{1a}$$
$$m\ddot{y} + F_y(x,y) = 0\,, \tag{1b}$$

where F_x and F_y describe the restoring forces of the springs in the x- and y-displacements respectively. These restoring forces lead to coupling between the x- and y-directions; however, as previously discussed, they do not generate a linear coupling force. Therefore, the linear modal coordinates may

[1] As this is a periodic response of the conservative system, this motion represents a nonlinear normal mode – i.e. a point on the backbone curve that emanates from the horizontal linear mode.

be written as $q_1 = mx$ and $q_2 = my$ which, when substituted into Eqs. (1) may be approximated to

$$\ddot{q}_1 + \omega_1^2 q_1 + \alpha_1 q_1^2 + \alpha_2 q_1 q_2 + \alpha_3 q_2^2 + \alpha_4 q_1^3 + \alpha_5 q_1^2 q_2 + \alpha_6 q_1 q_2^2 + \alpha_7 q_2^3 = 0\,, \quad (2a)$$

$$\ddot{q}_2 + \omega_2^2 q_2 + \beta_1 q_1^2 + \beta_2 q_1 q_2 + \beta_3 q_2^2 + \beta_4 q_1^3 + \beta_5 q_1^2 q_2 + \beta_6 q_1 q_2^2 + \beta_7 q_2^3 = 0\,, \quad (2b)$$

where the parameters are given in Table 1. Note that, for simplicity, the nonlinear terms have been truncated to the third (cubic) order, using a Taylor series expansion. Although this approximate model is no longer an exact reflection of the dynamics of the system, it does still exhibit the strong quasi-static coupling between the modes, which allows this effect to be investigated for a mathematically simple model.

Table 1. The coefficients of the equations of motion, Eqs. (2).

Coefficient	Value	Coefficient	Value
ω_1	10	ω_2	100
α_1	0	β_1	5×10^5
α_2	10^6	β_2	10^4
α_3	5000	β_3	0
α_4	5×10^7	β_4	0
α_5	0	β_5	-1.01×10^8
α_6	-1.01×10^8	β_6	0
α_7	0	β_7	5×10^5

2.2 Overview of nonlinear reduced-order modelling

A nonlinear reduced-order model has fewer degrees-of-freedom than the original, full-order system – in this case, Eqs. (2) are treated as the full-order system. The ROM must accurately reproduce the dynamic behavior of the full-order system over a specific region, such as a range of response frequencies. For the case of the simple oscillator, the region of interest is defined as responses in the vicinity of the first linear natural frequency[2]. The reduced-order modelling approach developed here assumes that the full-order equations of motion are unknown – which is often the case when a nonlinear structure is modeled using commercial FE software. Therefore, the reduction methodology should not require access to the full-order equations of motion. For the simple example considered here, the full-order equations of motion, Eqs. (2), are known, however these will not be explicitly used to calibrate the ROMs. Note that in §4 an FE model is used as a full-order model – a case where the full-order equations of motion are not known explicitly.

The reduced-order modelling procedure used here is the applied loads method, which is implemented as follows:

1. Select the modal basis and parametrised form of the nonlinear functions (a polynomial series is typically used).
2. Apply a series of static load cases to the full-order model. These loads should be applied to the modes that are included in the ROM.
3. Measure the modal displacements that result from these load cases for the modes included in the ROM.
4. Estimate the parameters of the nonlinear functions using the force and displacement data.

Note that the number of load cases must be equal to, or greater than, the number of unknown parameters in the nonlinear functions. Therefore, a larger ROM (i.e. with more degrees-of-freedom) or a higher-order of nonlinearity will require a larger number of load cases. Normally, the nonlinear function is described using a series of quadratic and cubic functions [11, 21] – i.e. higher-order polynomials are not typically included.

2.3 Motivating results for the simple oscillator

The applied loads method is now used to find ROMs describing the full-order model of the oscillator, Eqs. (2). As previously discussed, the responses in the region of the first linear natural frequency are of interest; hence the ROM consists of a single mode, q_1. A typical ROM, with nonlinearities up to the cubic order is therefore of the form

$$\ddot{q}_1 + \omega_1^2 q_1 + \gamma_2 q_1^2 + \gamma_3 q_1^3 = 0\,, \quad (3)$$

where parameters γ_2 and γ_3 are to be estimated (it is assumed that the linear natural frequency may be obtained separately). Equation (3) is referred to here as the 3$^{\text{rd}}$-order ROM and may be considered as the standard expansion used in the literature. An additional, and novel, ROM with nonlinear terms up to the 9$^{\text{th}}$ order is also used for comparison[3]. This is termed the 9$^{\text{th}}$-order ROM and is of the form

$$\ddot{q}_1 + \omega_1^2 q_1 + \gamma_2 q_1^2 + \gamma_3 q_1^3 + \gamma_4 q_1^4 + \gamma_5 q_1^5 + \gamma_6 q_1^6 + \gamma_7 q_1^7 + \gamma_8 q_1^8 + \gamma_9 q_1^9 = 0\,. \quad (4)$$

The 9$^{\text{th}}$-order ROM has six additional parameters that must be estimated and hence requires the computation of additional static solutions.

For both ROMs, the force-displacement data are obtained by applying static loads to the first mode (i.e. the only mode included in the ROMs) of the full-order model, i.e. solving

$$\omega_1^2 q_1 + \alpha_1 q_1^2 + \alpha_2 q_1 q_2 + \alpha_3 q_2^2 + \alpha_4 q_1^3 + \alpha_5 q_1^2 q_2 + \alpha_6 q_1 q_2^2 + \alpha_7 q_2^3 = F_S F_{q1}\,, \quad (5a)$$

$$\omega_2^2 q_2 + \beta_1 q_1^2 + \beta_2 q_1 q_2 + \beta_3 q_2^2 + \beta_4 q_1^3 + \beta_5 q_1^2 q_2 + \beta_6 q_1 q_2^2 + \beta_7 q_2^3 = 0\,, \quad (5b)$$

[2] As discussed later, the region of interest corresponds to NNMs represented by the first backbone curve of the system.

[3] The motivation for this particular order of ROM is described in §3.

for q_1 and q_2, where F_{q1} is the set of forces and F_S is the *force scale factor*. Here, the sets of forces are evenly spaced between -1 and $+1$, and match the number of unknown parameters in the 9$^{\text{th}}$-order model[4], i.e.

$$F_{q1} = \left\{-1, \frac{-5}{7}, \frac{-3}{7}, \frac{-1}{7}, \frac{1}{7}, \frac{3}{7}, \frac{5}{7}, 1\right\}. \tag{6}$$

These are then scaled using the force scale factor, F_S.

Once the displacements, resulting from the applied loads, have been found using the full-order model, the ROM parameters are estimated in a least-squares sense. For the 3$^{\text{rd}}$-order ROM, this involves finding γ_2 and γ_3 using the expression $\gamma_2 q_1^2 + \gamma_3 q_1^3 = F_S F_{q1} - \omega_1^2 q_1$, which may be achieved using

$$\begin{pmatrix} \gamma_2 \\ \gamma_3 \end{pmatrix} = \mathbf{A}^{-1}\mathbf{c_1}, \tag{7}$$

where the i^{th} rows of $\mathbf{A}$ and $\mathbf{c_1}$ are populated with the results of the i^{th} load case, i.e.

$$\mathbf{A} = \begin{pmatrix} \left[q_1^2,\, q_1^3\right]_{F_{q1}=-1} \\ \left[q_1^2,\, q_1^3\right]_{F_{q1}=-5/7} \\ \vdots \\ \left[q_1^2,\, q_1^3\right]_{F_{q1}=+1} \end{pmatrix}, \tag{8a}$$

$$\mathbf{c_1} = \begin{pmatrix} \left[F_S F_{q1} - \omega_1^2 q_1\right]_{F_{q1}=-1} \\ \left[F_S F_{q1} - \omega_1^2 q_1\right]_{F_{q1}=-5/7} \\ \vdots \\ \left[F_S F_{q1} - \omega_1^2 q_1\right]_{F_{q1}=+1} \end{pmatrix}. \tag{8b}$$

A similar expression is used to find the parameters of the 9$^{\text{th}}$-order ROM, where $\mathbf{A}$ and $\mathbf{c_1}$ measure $\{8\times 8\}$ and $\{8\times 1\}$ respectively.

Figure 4 shows how the cubic parameter, γ_3, of the 3$^{\text{rd}}$- and 9$^{\text{th}}$-order ROMs varies with the force scale factor, F_S. The maximum force scaling factor considered here, $F_S = 0.16$, corresponds to an absolute static displacement of approximately 0.17 ℓ_1 and 0.02 ℓ_2 in the x- and y-directions respectively. As previously noted in studies of the applied loads procedure, [2, 22], the parameters of the system are dependent on the force scale factor. This is clearly seen in Fig. 4 where, for the 3$^{\text{rd}}$-order ROM, γ_3 varies significantly. As a result, the force scale factor must be carefully chosen to obtain an accurate model of the system. This large variation in γ_3 illustrates a fundamental issue with the structure of the function used to approximate the nonlinear restoring forces in the ROM. The cubic parameter of the 9$^{\text{th}}$-order ROM, however, appears to be less sensitive, implying that this model is more robust to this choice of force scale factor. Note that, typically, only one force scale factor is chosen to calibrate the ROM – multiple scale factors are used here to demonstrate the effect of this choice on the parameter values.

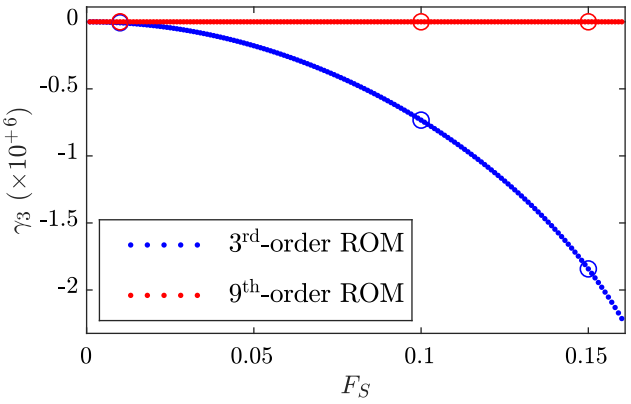

Fig. 4. The effect of force scale factor, F_S, on the cubic parameter, γ_3, of the two ROMs. Note that each dot represents a γ_3 value for a given force scale factor. The circles denote specific force scale factors, at $F_S = \{0.01, 0.1, 0.15\}$, that are used to compute the backbone curves shown in Fig. 5.

A backbone curve is a locus of conservative, periodic responses (i.e. a locus of nonlinear normal modes) and captures the fundamental dynamic behavior of a nonlinear system [23]. As such, backbone curves may be used as a means of assessing the accuracy of ROMs [22]. The backbone curve of the two ROMs, calibrated using three different scale factors, are shown in Fig. 5[5]. These are compared to the first backbone curve (i.e. the backbone curve emerging from the first linear natural frequency) of the full-order model. It is clear that the 9$^{\text{th}}$-order ROMs are more accurate than the 3$^{\text{rd}}$-order ROMs. Additionally, as indicated in Fig. 4, the 9$^{\text{th}}$-order ROMs are significantly more robust to the choice of force scale factor – at this scale, it is difficult to differentiate between these backbone curves. As shown in Fig. 4, the cubic parameter of the 3$^{\text{rd}}$- and 9$^{\text{th}}$-order ROMs becomes equivalent at low force scale-factors, demonstrating that the difference between the backbone curves of these ROMs is driven by the higher-order terms (considered in detail in the following section). These results motivate the need for higher-order nonlinear terms in the ROM.

Recalling that the nonlinearities of the full-order system, Eqs. (2), are truncated at the third order, it may seem counter-intuitive that the dynamics are best captured by a 9$^{\text{th}}$-order ROM. The following section explores how the quasi-static coupling between the two modes leads to a ROM that requires a higher-order of nonlinearity than the full-order system.

[4]Note that, typically, ROMs are calibrated using a minimum number of load cases, e.g. 2 for a single-DOF 3$^{\text{rd}}$-order ROM. However, here each ROM utilises 8 load cases, which allows for a direct comparison between ROMs of different orders.

[5]These have been computed using the MATLAB®-based numerical continuation software Continuation Core (COCO) [9].

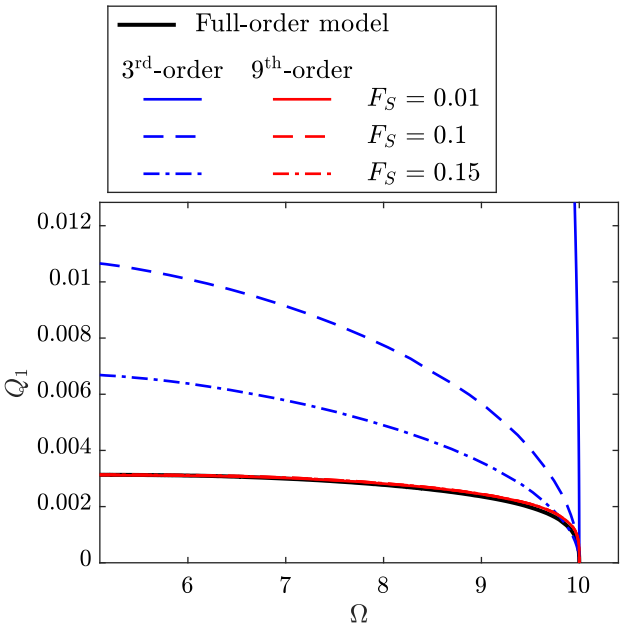

Fig. 5. A comparison between the two ROMs, calibrated using different force scale factors, F_S, using the first backbone curve. These are compared to the first backbone curve of the full-order model, represented by the solid-black line. The blue and red lines represent the 3rd- and 9th-order ROMs respectively, whilst the solid, dashed and dotted-dashed lines denote the three different force scale factors used to calibrate the ROMs. These are shown in the projection of the response frequency, Ω, against the amplitude of displacement of the first mode, Q_1. The response frequency is defined as $\Omega = 2\pi T^{-1}$, where T is the period of the response, and the displacement amplitude is defined as $Q_1 = (\max\{q_1\} - \min\{q_1\})/2$.

3 Accounting for quasi-static coupling in nonlinear reduced-order models

3.1 The effect of quasi-static coupling on the order of nonlinear terms

When a force is applied in the first mode of the 2-DoF oscillator, the resulting static deflection in the first mode is accompanied by a static deflection in the highly stiff second mode, such that the oscillator follows an arced path, as previously illustrated in Fig. 3. This modal coupling may be approximated as quasi-static, i.e. the second mode may respond dynamically[6], but is constrained by the stiffness coupling with the first mode, which may be captured statically. Reducing the order of the full model[7] therefore cannot rely on the assumption that q_2 is small – i.e. removing all q_2-dependent terms in the full-order q_1 equation (Eq. (2a)) will not lead to an accurate ROM. Instead, reducing the order of Eqs. (2) relies on the assumption that the inertial term, $\ddot{q}_2$, is small in relation to the stiffness components in the second modal equation of motion, Eq. (2b). This allows the *dynamics* of the second mode to be neglected, without requiring the displacement to be negligible. When the second linear natural frequency is significantly larger than the first, i.e. $\omega_2 \gg \omega_1$, this assumption is reasonable, and does not require q_2 to be small in relation to q_1. By assuming that $\ddot{q}_2 \approx 0$ (as is done when the loads are applied to the static system in Eqs. (5)), the second equation of the static full-order system, Eq. (5b), allows the second mode to be written as a function of q_1, i.e.

$$q_2 = f(q_1, \omega_2, \beta_1, \beta_2, \ldots), \tag{9}$$

where ω_2 and β_i are the second linear natural frequency and nonlinear parameters of Eq. (5b), respectively. This may be approximated to a J^{th}-order polynomial function of q_1, i.e.

$$q_2 \approx \sum_{j=2}^{J} A_j q_1^j, \tag{10}$$

where $A_j = A_j(\omega_2, \beta_1, \beta_2, \ldots)$, i.e. the constants A_j depend upon the second linear natural frequency and nonlinear parameters but are independent of the force applied to the system or q_1. As such, the values A_j may be considered fixed for a given set of system parameters. Note that no linear term is included in Eq. (10) as q_1 and q_2 must, by definition, be linearly independent. Substituting Eq. (10) into the first equation of the full-order model, Eq. (2a), leads to the ROM

$$\ddot{q}_1 + \omega_1^2 q_1 + \sum_{j=2}^{3J} \gamma_j q_1^j = 0, \tag{11}$$

where

$$\gamma_2 = \alpha_1, \tag{12a}$$
$$\gamma_3 = \alpha_4 + A_2\alpha_2, \tag{12b}$$
$$\gamma_4 = A_2\alpha_5 + A_2^2\alpha_3 + A_3\alpha_2, \tag{12c}$$
$$\gamma_5 = A_2^2\alpha_6 + 2A_2A_3\alpha_3 + A_3\alpha_5 + A_4\alpha_2, \tag{12d}$$
$$\gamma_6 = A_2^3\alpha_7 + 2A_2A_3\alpha_6 + 2A_2A_4\alpha_3 + A_3^2\alpha_3 + A_4\alpha_5 + A_5\alpha_2, \tag{12e}$$
$$\gamma_7 = 3A_2^2A_3\alpha_7 + 2A_2A_4\alpha_6 + 2A_2A_5\alpha_3 + A_3^2\alpha_6 + 2A_3A_4\alpha_3 + A_5\alpha_5 + A_6\alpha_2, \tag{12f}$$
$$\vdots \quad \vdots$$

Note that when $J = 3$, Eq. (11) is the same as the 9th-order ROM considered earlier, Eq. (4).

Equations (12) show that the ROM parameters, γ_i, are only dependent on the quasi-static coupling parameters[8], A_j, and the nonlinear parameters, α_k. As such, the ROM parameters are *independent of the force scale factor*. This demonstrates that the ROM is fixed for the system and should not

[6] In the presence of a dynamic interaction (e.g. internal resonance), the participating modes must be included as independent DoFs in the ROM.

[7] Note that here we define the *order* of the nonlinearity as the maximum order of the polynomial in the restoring forces.

[8] The term *quasi-static coupling parameter* is adopted here as the *quasi-static coupling function*, Eq. (10), reflects the assumption of quasi-static coupling between the modes.

vary with the force scale factor. It should also be highlighted that this ROM has a significantly higher-order of nonlinearity than the full-order equations of motion (recalling that the nonlinear terms in the full-order model do not go beyond the cubic order). Furthermore, assuming that q_2 is a function of q_1, will *always* lead to a higher-order polynomial in the ROM, as this quasi-static coupling function must be nonlinear.

For this simple, 2-DoF system, the ROM parameters, γ_i, may be computed directly. From Eqs. (12), these require the parameters A_j, which, as previously discussed, may be computed using the second equation of motion of the full-order model, Eq. (2b), and assuming that the inertial term is negligible. Note that this would not be practical for larger, more complex systems, and would not be possible for FE models where the full-order equations of motion are not accessible.

As the lowest order of nonlinearity in the full-order system is quadratic, the quasi-static coupling parameter A_j cannot contribute to the parameter γ_i where $i < j+1$. This can be seen in Eqs. (12), where A_2 does not contribute to γ_2, and A_3 does not contribute to γ_2 or γ_3, etc. As such, the ROM parameters up to γ_9 can be computed precisely by finding q_2 as a function of q_1 up to order $J = 8$, from Eq. (10). These parameters are given in Table 2.

Table 2. Values of parameters for the function of q_2 in terms of q_1, Eq. (10), and the general reduced-order model, Eq. (11).

A_j	Value	γ_j	Value
A_2	-50	γ_2	0
A_3	50	γ_3	0
A_4	-5.051×10^{5}	γ_4	6.250×10^{7}
A_5	1.010×10^{6}	γ_5	-7.576×10^{11}
A_6	-5.096×10^{9}	γ_6	1.768×10^{12}
A_7	1.528×10^{10}	γ_7	-1.020×10^{16}
A_8	-5.129×10^{13}	γ_8	3.440×10^{16}
		γ_9	-1.285×10^{20}

Table 2 shows that the quadratic and cubic parameters, γ_2 and γ_3, of the reduced-order model are both zero. Recalling that the full-order equations of motion contain quadratic and cubic terms, this may seem surprising and further highlights the importance of including higher-order terms for fitting. This also demonstrates why, for low scale factors, the 3rd-order ROM tends towards a linear system, as seen in Fig. 5. Note, however, that $\gamma_2 = \gamma_3 = 0$ is not a feature that is common to all ROMs as seen in §4, where a beam with clamped end-conditions is considered.

In all but the simplest of systems it is not practical to compute the ROM coefficients by directly solving the unmodeled modes in terms of the modes retained in the ROM, and for many FE models it is not possible to access the equations of motion. For more complex systems these parameters may still be estimated using the least-squares fit, shown previously in §2.3, which will require a truncation of the order of the nonlinearity in the ROM. This will introduce an error, which is likely to increase as the force scale factor is increased (as the neglected higher-order terms will become, relatively, more significant as the displacement increases). However, this may be viewed as an *approximation error*, rather than a *tuning* of the model, as the "target" γ_i are invariant with force scale factor.

3.2 Reduced-order models of the simple oscillator

Figure 6 shows the relative errors between the true (i.e. using Eq. (12)) and estimated parameters (using Eqs. (7) and (8)) of the 3rd- and 9th-order ROMs. These errors are defined as $(\hat{\gamma}_i - \bar{\gamma}_i)/\bar{\gamma}_i$, where $\bar{\gamma}_i$ and $\hat{\gamma}_i$ denote the true and estimated values of γ_i respectively. As $\bar{\gamma}_2 = \bar{\gamma}_3 = 0$, the estimated values, rather than the relative errors, of $\hat{\gamma}_2$ and $\hat{\gamma}_3$ are shown. Also note that the plot of the estimated values of γ_3, for the two different ROMs, was shown previously in Fig. 4.

Figure 6 further demonstrates that the 9th-order ROM is significantly more robust to the force scale factor, F_S, than the 3rd-order model. However, Fig. 6 does reveal that there is some error associated with the estimation of the 9th-order parameters, and that this error increases with F_S. As previously discussed, this is due to the higher-order terms becoming, relatively, more significant at higher force scale factors. The magnitude of these errors appears to increase with the order of the term; however, for the range of force scale factors considered here, these errors remain small. This is because the relative significance of the corresponding polynomial term is small, as discussed in the following section and shown in Fig. 8. Assuming that the terms above the 9th-order are negligible, this suggests that the 9th-order fit should give consistently accurate results, even at low force scale factors.

Estimating γ_i by fitting F_{q1} to a polynomial function of q_1 (using, for the 3rd-order case, Eqs. (7) and (8)) allows the ROM to be formulated and the responses of the modes captured by the ROM (q_1 in this example) to be computed. As with the Implicit Condensation and Expansion method, introduced by Hollkamp and Gordon [21], an additional step allows the dynamics of the unmodeled modes (q_2 in this instance) to be estimated. This requires the parameters, A_j, of the quasi-static coupling function, Eq. (10). These may be estimated using the displacements q_2 that result from static load cases applied to q_1 – note that the first step where the parameters γ_i are found, used the first modal displacements, q_1, but disregarded the second mode, q_2. Therefore, the parameters A_j may be estimated without the need for any additional load cases and, for the 3rd-order ROM, this may be computed using

$$\begin{pmatrix} A_2 \\ A_3 \end{pmatrix} = \mathbf{A}^{-1}\mathbf{c_2}\,, \tag{13}$$

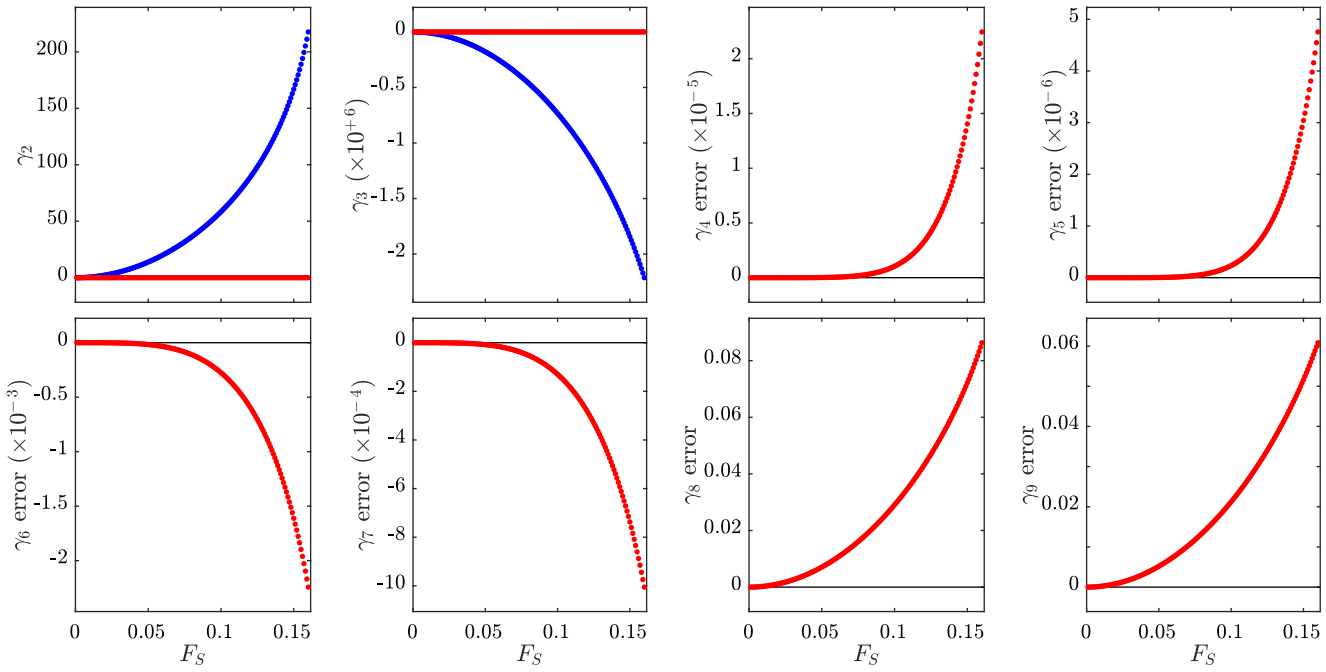

Fig. 6. The values and relative errors of the estimated parameters of the 3rd- and 9th-order ROMs, represented by blue and red dots respectively. These are shown in the projection of the force scale factor, F_S, against the value or relative error of the ROM parameter, γ_i. The true values of parameters γ_2 and γ_3 are zero (see Table 2) and hence the estimated values, rather than relative errors, are shown. All remaining panels, for $\gamma_{4\to 9}$, show the relative errors of the estimated values.

where

$$\mathbf{c_2} = \begin{pmatrix} [q_2]_{F_{q1}=-1} \\ [q_2]_{F_{q1}=-5/7} \\ \vdots \\ [q_2]_{F_{q1}=+1} \end{pmatrix}, \tag{14}$$

and $\mathbf{A}$ is as defined in Eq. (8). A similar expression is used for the 9th-order ROM.

Figure 7 shows the first backbone curve of the oscillator in terms of the amplitudes of the first and second modes, Q_1 and Q_2 respectively. The projection of the first modal amplitude, in Fig. 7(a), was shown previously in Fig. 5. In Fig. 7(b), q_2 has been found using a 3rd- and 9th-order polynomial fit (for the 3rd- and 9th-order ROMs respectively) to q_1 – i.e. Eq. (10). The values of parameters A_j differ between the force scale factors and ROMs. As previously discussed for the Q_1-projection, the backbone curve of the 9th-order ROMs (red lines in Fig. 7(a)) show a much better agreement with that of the full-order model (black line) than that of the 3rd-order ROMs (blue lines). This trend is also seen in the projection of the second modal amplitude, Q_2, shown in Fig. 7(b). In both projections, the backbone curves of the 9th-order ROMs overlap, demonstrating the robustness of the fit of q_2 with respect to the force scale factor, F_S. It should be acknowledged that, to some degree, it is unsurprising that higher-order expressions enable a better fit; however, it is the physical justification for this that is paramount.

3.3 Comparing the accuracy of different orders of nonlinear reduced-order models

The 9th-order ROM has been shown to give significantly more accurate backbone curve results, and a significant increase in robustness to force scale factor, in comparison to the 3rd-order ROM. This demonstrates the advantages of selecting a high order of nonlinearity in the reduced-order model, even when the full-order model has a relatively low order of nonlinearity. As previously discussed, the 9th-order of nonlinearity captures the effects of all terms in the quasi-static coupling function, Eq. (10), up to the third order, i.e. for $J = 3$. However, it has also been noted that the terms in the ROM with a very high order are likely to be less significant. This implies that a lower-order of nonlinearity (i.e. less than 9th-order) in the ROM may still be able to accurately capture the dynamics of the full-order system. This is firstly investigated by inspecting the magnitudes of the terms in the 9th-order ROM at different response amplitudes.

Figure 8 compares the magnitudes of the polynomial terms for three different points on the backbone curve. The magnitude of the n^{th}-order term is calculated as $\max\{|\gamma_n q_1^n|\}$, where the true value of γ_n is used, from Table 2, and the backbone curve is computed using the full-order model. The labels on the axes of the inset panels denote the term order. Note that the 2nd- and 3rd-order terms are not shown as $\gamma_2 = \gamma_3 = 0$, hence their magnitudes must be zero. Figure 8 clearly demonstrates that, for the three points shown here, the 5th-order term is dominant. The 7th-order term becomes more significant at higher amplitudes, whilst the 9th-order term is negligible at lower amplitudes, and very small

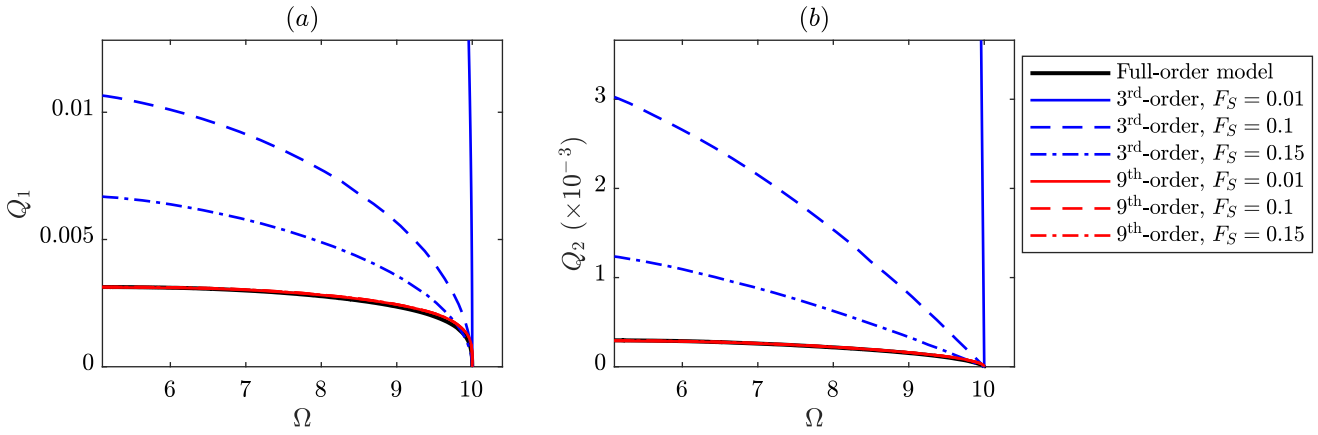

Fig. 7. A comparison between the two ROMs, calibrated using different force scale factors (F_S) using the first backbone curve. These backbone curves are shown in the projection of response frequency, Ω, against the first and second modal displacement amplitudes, Q_1 and Q_2, in panels (a) and (b) respectively. These modal amplitudes are defined as $Q_i = (\max\{q_i\} - \min\{q_i\})/2$. These are compared to the first backbone curve of the full-order model, represented by the solid-black line. The blue and red lines represent the 3rd- and 9th-order ROMs respectively.

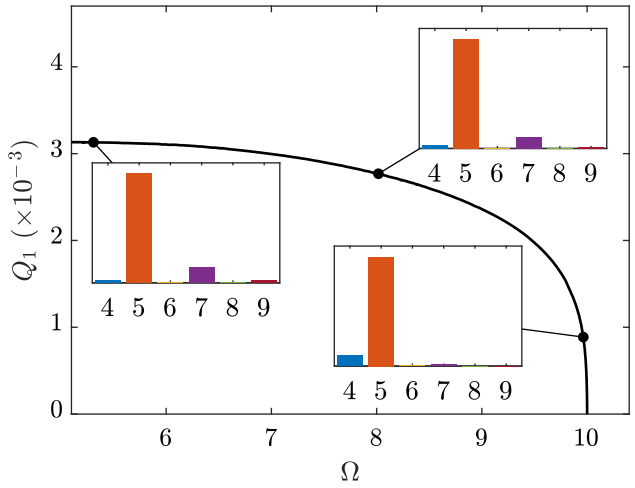

Fig. 8. A comparison of the relative magnitudes of the nonlinear terms in the ROM, for three different points on the backbone curve. The black line shows the backbone curve of the full-order system and the three black dots denote the three responses used for comparison. The inset panels show the relative magnitudes of the terms, for terms 4 to 9, where the n^{th} term is given by $\gamma_n q_1^n$.

at higher amplitudes. Of the even-valued terms, the 4th-order term is relatively significant, particularly at low amplitudes, whilst the 6th- and 8th-order terms are negligible for all three points shown[9].

The observation that the high-order terms appear to be small, from Fig. 8, implies that a lower-order (i.e. lower than 9th-order, but higher than 3rd-order) ROM may give good accuracy. This is now investigated by comparing all orders of ROM, from the 3rd to the 9th. As before, each ROM uses 8 evenly distributed load cases.

Figure 9 shows the backbone curves predicted by ROMs of different orders, all found using a force scale factor of $F_S = 0.1$. Panels (a_1) and (a_2) compare the 3rd- and 4th-order ROMs, represented by dashed-blue and solid-red lines respectively, to the full-order model, represented by a solid-black line. These results show that the addition of the 4th-order term only allows for a small improvement to the accuracy of the backbone curve. This is to be expected as, from Fig. 8, the 5th-order term is the most significant term but is not included in either the 3rd- or 4th-order ROMs.

Figures $9(b_1)$ and $9(b_2)$ compare the first backbone curve of the 5th- to the 9th-order ROMs to that of the full-order model. These are significantly more accurate than the 3rd- and 4th-order ROMs, shown in Figs. $9(a_1)$ and $9(a_2)$. This is primarily due to the presence of a 5th-order nonlinear term (previously identified as the most significant term) in all ROMs of order 5 and above. Comparing the 5th- and 6th-order ROMs reveals that the addition of the 6th-order term results in a small change – reflecting the observation from Fig. 8 that the 6th-order term is negligible. Likewise, the 7th- and 8th-order backbone curves are indistinguishable, as the 8th-order term is also negligible. As the 7th-order term is significant, however, the 7th-and 8th-order ROMs do show a significant improvement compared to the lower orders. Finally, the 9th-order ROM leads to an improvement in accuracy; however, this improvement is minor, due to the size of the 9th-order term.

From this it can be concluded that, whilst the 9th-order ROM is required to fully-capture the cubic description of q_2 in terms of q_1 (i.e. for $J = 3$), the effect of the 9th-order term is negligible. A very good fit in the backbone curve may still be achieved with a 7th-order model, and a 5th-order model also provides a good fit. Overall, this demonstrates that a higher-order will lead to a greater accuracy but, if a lower-order is desired (for example, if a limited number of load cases, and hence parameters, are available) then a good accuracy may still be achieved.

In summary, this section has demonstrated that the

[9]Note that this analysis requires the true solution to be known, and hence cannot typically be applied prior to estimating the terms.

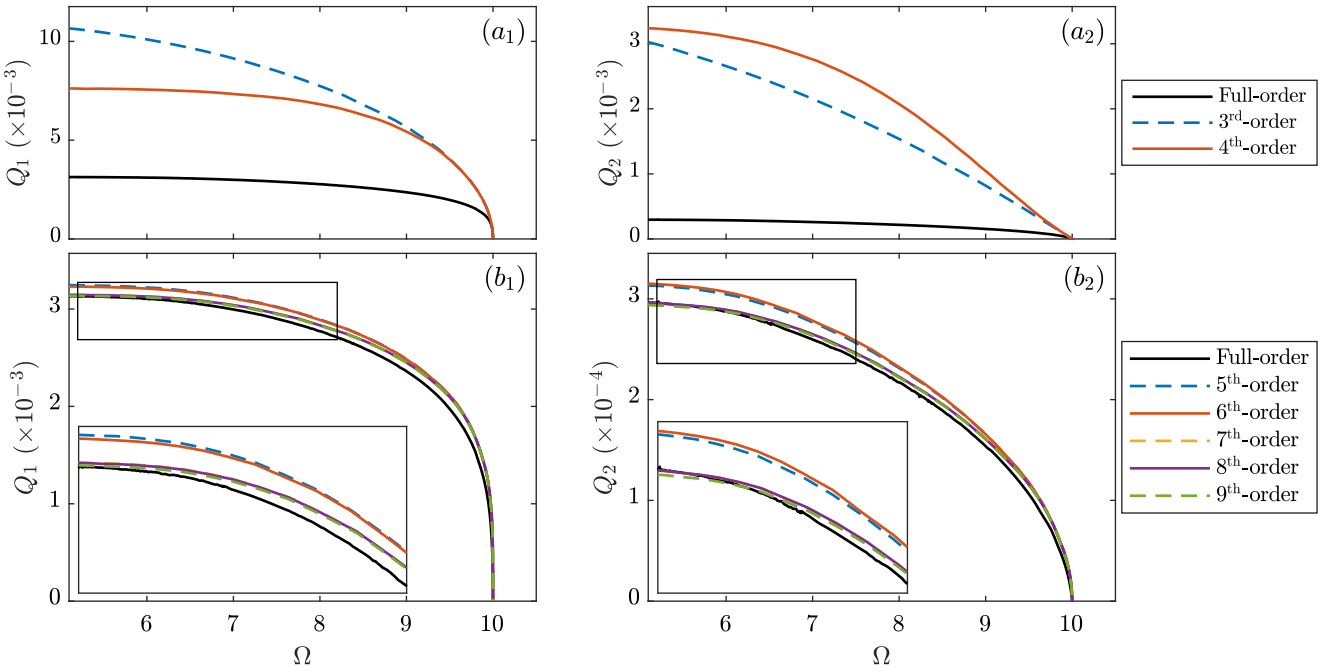

Fig. 9. A comparison between the backbone curves of different order ROMs. The 3rd- and 4th-order ROMs are compared to the full-order model in panels (a_1) and (a_2) – shown in the projection of frequency, Ω, against the first and second modal amplitudes, Q_1 and Q_2, respectively. Similarly, the 5th-to-9th-order ROMs are compared to the full-order models in panels (b_1) and (b_2). These ROMs have been computed using a force scale factor of $F_S = 0.1$.

quasi-static coupling between the two linear modes of the simple, 2-DoF oscillator leads to a higher-order of nonlinearity in the ROM than in the full-order equations of motion. Whilst a higher-order ROM does require additional parameters for fitting, it is significantly more robust to the force scale factor and produces significantly more accurate backbone curves for the case considered here. The following section extends this analysis to a clamped-clamped beam, modeled using the FE software Abaqus [12].

4 Application to a finite element model

The 3rd- and 9th-order single-mode ROMs of a geometrically nonlinear clamped-clamped beam, modeled using the FE software Abaqus [12], are now considered. The beam has a length, width and height (h) of 650 mm, 30 mm and 2 mm respectively, and is constructed of steel with a Young's modulus, shear modulus and density of 210 GPa, 80 GPa and 7850 kg m^{-3} respectively. The beam is modeled using 130 beam elements of type B32 [12], resulting in 1554 DoFs. Its first mode, which is the only mode retained in the ROMs, corresponds to the first bending mode of the beam and has a linear natural frequency of $\omega_1 \approx 158$ rad s^{-1}. Note that the single-mode ROMs computed here, aim to capture the salient behavior of the beam in the vicinity of the first nonlinear normal mode, and are used to investigate the coupling between the low-frequency (bending) and high-frequency (axial) modes – they are not intended to fully describe the dynamics of the system, for example by capturing dynamic interactions such as internal resonances.

The static solution data used to construct the ROMs were obtained by applying a static force proportional to the first modeshape, and projecting the resulting physical displacement of the beam, onto the mass-normalised linear modeshapes. Similar to the approach described in §2.3, both the 3rd- and 9th-order ROMs constructed for each force scale factor (F_S), utilise 8 pairs of force-displacement data, in which the reduced modal force applied to the beam is equally distributed between $-F_S$ and $+F_S$. The minimum force scale factor considered here, $F_S = 8.7$, corresponds to the force required to achieve a maximum displacement of ~ 1 mm $= 0.5h$ in the underlying linear system. This value was found to produce optimal results for a single-mode ROM of a clamped-clamped beam in [22], where the sensitivity to the scaling factor was demonstrated using Gordon and Hollkamp's [2] *Constant Linear Displacement* method of scaling. The maximum force scale factor considered here, $F_S = 100$, extends beyond the optimal value, and corresponds to a linear maximum displacement of ~ 11.5 mm $= 5.75h$, and an actual (nonlinear) maximum displacement ($w_{\max}$) of ~ 3.64 mm $= 1.82h$.

4.1 Modal coupling

Figure 10 shows the displacement of the first mode, q_1, against the displacements of two axial modes, q_{59} and q_{101} – i.e. the 59th and 101st modes. These modal displacements are reached when forces are applied in only the first mode, hence the axial displacements are only triggered due to the coupling with the first mode. As these modes are significantly stiffer than the first (i.e. $\omega_{59}/\omega_1 \approx 316$ and $\omega_{101}/\omega_1 \approx 632$),

this coupling may be assumed to be quasi-static, as seen in the simple oscillator considered previously. There is a clear similarity between the free periodic response of the simple oscillator, shown previously in Fig. 3, and the modal displacements in Fig. 10.

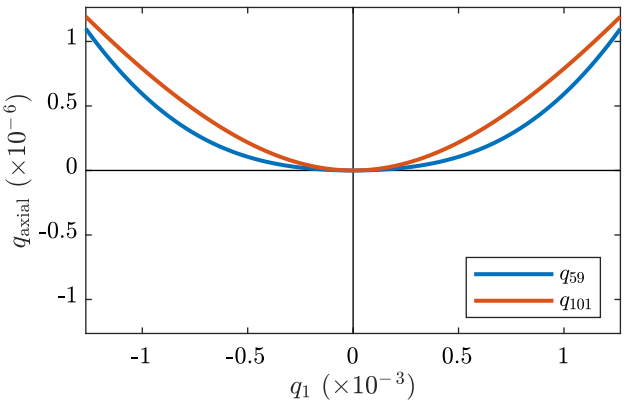

Fig. 10. The static displacements of the first bending mode (q_1) and two axial modes (q_{59} and q_{101}) when the structure is subjected to forces in the first mode.

Figure 11 shows the corresponding energy of the two axial modes as a percentage of the energy of the first mode, plotted against the displacement of the first mode[10]. These are calculated using a linear energy integral, i.e. $E_n = 0.5\omega_n^2 q_n^2$, for $n = 1, 59, 101$. Even though the force was only applied to the first mode of the beam, the amount of energy induced in the highly stiff axial modes is relatively large. This highlights the significance of the axial modes in the response of the beam, even when operating at frequencies much lower than their natural frequencies.

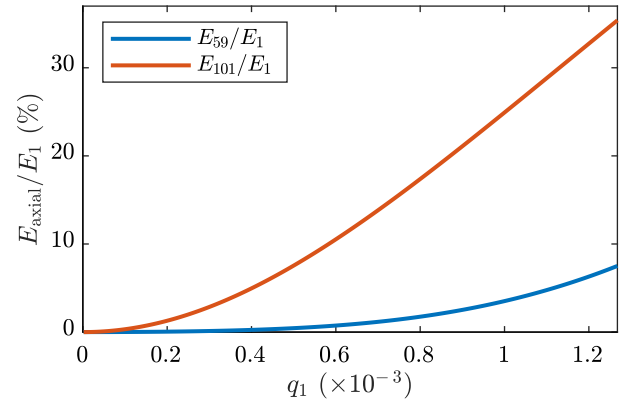

Fig. 11. The ratio of the energy of two axial modes (E_{59} and E_{101}) to the energy of the first mode (E_1), plotted against the static displacement of the first mode.

[10] As the response of the axial modes is symmetric, only positive displacements are shown here.

4.2 Single-mode reduced-order model results

Figure 12 shows the estimated parameters of the 3rd- and 9th-order ROMs of the clamped-clamped beam for force scale factors in the range $F_S = [8.7, 100]$. The top-left panel shows that both the 3rd- and 9th-order ROMs predict a quadratic parameter, γ_2, that is close to zero, regardless of the scale of the load applied. This is expected, as the structure is symmetric.

The cubic parameter, γ_3, of the 3rd-order ROM (represented by blue dots) varies significantly as the force scale factor is increased. The cubic parameter in the 9th-order ROM, meanwhile, remains close to a fixed value, suggesting that it is less sensitive to the force scale factor. This agrees with the findings of the simple oscillator, considered in previous sections.

The even-valued parameter γ_4 (only present in the 9th-order ROM) fluctuates around relatively small values[11]. The term corresponding to this parameter may be considered negligible, which, again, is expected due to the symmetric nature of the beam.

In contrast, the odd-valued parameter γ_5 is more than 10 orders of magnitude larger than γ_4, and the trend it exhibits is qualitatively similar to that of γ_3. The significance of this term is also later verified in Fig. 14, further justifying the need for nonlinear terms of order higher than cubic. Given the magnitude of the quintic monomial in the ROM, relative to the cubic one, the effect of the variation in γ_5 is small, resulting in a robust ROM as the force scale factor varies.

Figure 13 shows a comparison of the backbone curves of the 3rd- and 9th-order ROMs, calibrated using three different force scale factors ($F_S = \{8.7, 50, 100\}$). Note that, as the backbone curve of the full-order FE model is unknown, it is not compared to that of the ROMs in this case. The figure demonstrates the sensitivity of the 3rd-order ROMs to the force scaling factor, which can lead to inaccurate response predictions when the proper scaling is not chosen. In contrast, the 9th-order ROMs result in backbone curves that remain practically indistinguishable as the scale factor varies.

It should also be highlighted that the 9th-order ROMs produce results similar to those obtained using the optimal 3rd-order ROM ($F_S = 8.7$), as reported in [22]. This highlights the accuracy, as well as robustness of the 9th-order ROMs, which can eliminate the need for detailed tuning of the scaling factor for each specific application.

Figure 14 shows the backbone curve predicted by the 9th-order ROM, calibrated using a force scale factor of $F_S = 100$. Similarly to Fig. 8, the inset panels represent the magnitude of the nonlinear term for three different points on the backbone curve. The figure demonstrates that the cubic terms are dominant in all three responses, which largely justifies the use of 3rd-order ROMs in similar studies in the literature, especially for lower response amplitudes. However, it is highlighted that the odd-valued higher-order nonlinearities become increasingly significant at higher amplitudes. This indicates that, as with the simple oscillator, a ROM with an

[11] Note that, whilst $\gamma_4 = O(10^4)$, the corresponding ROM term will be insignificant, i.e. $\gamma_4 q_1^4 = O(10^{-8})$, since $q_1 = O(10^{-3})$.

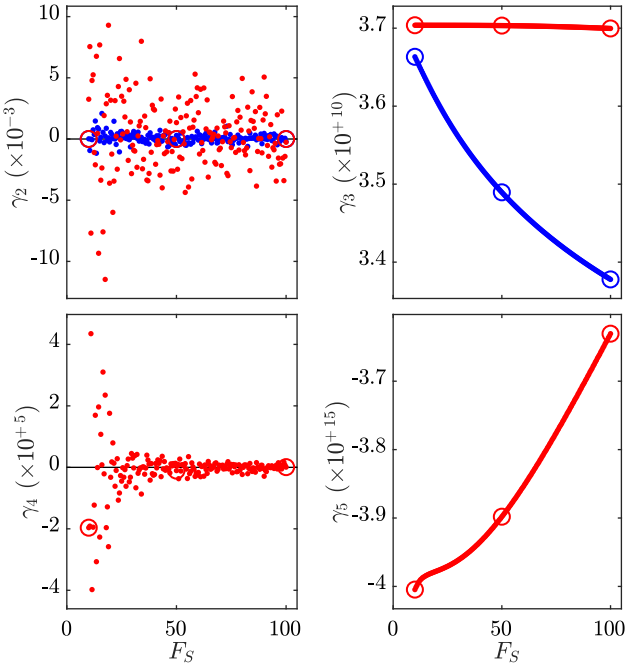

Fig. 12. The values of the estimated parameters of the 3rd- and 9th-order ROMs, represented by blue and red dots respectively. These are shown in the projection of the force scale factor, F_S, against the value of the ROM parameter, γ_i. The circles denote specific force scale factors, at $F_S = \{8.7, 50, 100\}$, that are used to compute the backbone curves shown in Fig. 13.

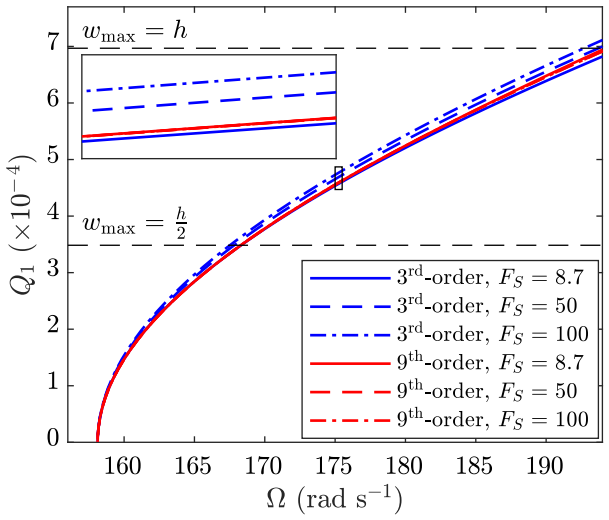

Fig. 13. A comparison between the two ROMs, calibrated using different force scale factors, F_S, using the first backbone curve. The blue and red lines represent the 3rd- and 9th-order ROMs respectively, whilst the solid, dashed and dotted-dashed lines denote the three different force scale factors used to calibrate the ROMs.

order of nonlinearity that is higher than 3rd-order is required to robustly and accurately capture the backbone curve at high amplitudes.

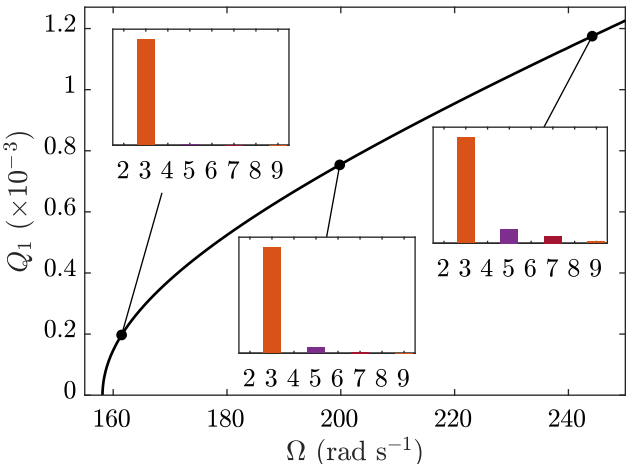

Fig. 14. A comparison of the relative magnitudes of the nonlinear terms in the ROM, for three different points on the backbone curve. The black line shows the backbone curve of the 9th-order ROM and the three black dots denote the three responses used for comparison. The inset panels show the relative magnitudes of the terms, for terms 2 to 9, where the n^{th} term is given by $\gamma_n q_1^n$.

5 Conclusions

This paper has demonstrated that the dynamic coupling between high- and low-frequency modes of a system can be approximated as a *quasi-static* interaction. If this coupling is sufficiently strong, the effect of the high-frequency modes must be accounted for in the reduced-order models of the low-frequency modes; however, they do not need to be modeled as independent DoFs. Specifically, it has been shown that quasi-static coupling introduces higher orders of nonlinearity in the ROMs, beyond the order of nonlinearity present in the full-order model. It has been demonstrated that including higher-order nonlinear terms leads to a significant increase in the accuracy of the ROMs – determined by comparing the backbone curves of a conceptually simple, 2-DoF oscillator. Furthermore, these higher-order ROMs are significantly more robust to the force scale factor used to calibrate the parameters of the ROMs. These findings have also been validated by computing ROMs of a clamped-clamped beam, modeled using commercial FE software.

Although ROMs with higher orders of nonlinearity are computationally more expensive to calibrate, their invariance to force scale factor makes them more robust and removes the need for any *tuning* of the force scale factor. Additionally, higher force scale factors may be used to calibrate these ROMs, thus removing the need to extrapolate the responses of the models beyond their calibrated domain. This further adds to the robustness and trustworthiness of the higher-order ROMs. Future work will include investigating the robustness of the quasi-static coupling approximation for the case where the frequencies of the modes are less separated.

Acknowledgements

The authors would like to thank Dr. Robbie Cook for his valuable discussions regarding FE modelling, and Mr. Thomas Wilkinson for his help in building the FE models. V.R.M. would like to acknowledge the support of the University of Bristol Alumni Foundation and the University of Bristol Faculty of Engineering. E.N., T.L.H. and S.A.N. would also like to acknowledge the support of the EPSRC via Programme Grant EP/R006768/1.

References

[1] Blevins, R.D., Holehouse, I., Wentz, K.R., 1993, "Thermoacoustic loads and fatigue of hypersonic vehicle skin panels," *J. Aircraft*, **30**(6), pp. 971–978.

[2] Gordon, R.W., Hollkamp, J.J., 2011 "Reduced-order models for acoustic response prediction," Tech. Rep. AFRL-RB-WP-TR-2011-3040, Air force research laboratory.

[3] Shearer, C.M., Cesnik, C.E., 2007, "Nonlinear flight dynamics of very flexible aircraft". *J. Aircraft*, **44**(5), pp. 1528–1545.

[4] Nayfeh, A.H., Mook, D.T., 1991, *Nonlinear Oscillations*, Wiley, Weinheim, Germany.

[5] Nayfeh, A.H., 2011, *Introduction to perturbation techniques*, John Wiley & Sons.

[6] Jezequel, L., Lamarque, C.H., 1991, "Analysis of nonlinear dynamical systems by the normal form theory," *J. Sound Vib.*, **149**(3), pp. 429–459.

[7] Hill, T.L., Neild, S.A., Cammarano, A. 2016, "An analytical approach for detecting isolated periodic solution branches in weakly nonlinear structures," *J. Sound Vib.*, **379**, pp. 150–165.

[8] Doedel, E.J., A. R. Champneys, Fairgrieve, T.F., Kuznetsov, Y.A., Dercole, F., Oldeman, B.E., Paffenroth, R.C., Sandstede, B., Wang, X.J., Zhang, C., 2007, "AUTO-07P: Continuation and Bifurcation Software for Ordinary Differential Equations".

[9] Schilder, F., Dankowicz, H., 2015, "Continuation Core (COCO)", accessed June 1, 2019, http://sourceforge.net/projects/cocotools/.

[10] Kuether, R.J., 2014, "Nonlinear modal substructuring of geometrically nonlinear finite element models," Ph.D. thesis, The University of Wisconsin-Madison.

[11] Mignolet, M.P., Przekop, A., Rizzi, S.A., Spottswood, S.M., 2013, "A review of indirect/non-intrusive reduced order modeling of nonlinear geometric structures," *J. Sound Vib.*, **332**(10), pp. 2437–2460.

[12] Dassault Systèmes, 2017, ABAQUS Documentation, Providence, RI, USA.

[13] Muravyov, A.A., Rizzi, S.A., 2003, "Determination of nonlinear stiffness with application to random vibration of geometrically nonlinear structures," *Comput. Struct.*, **81**(15), pp. 1513–1523.

[14] Rizzi, S.A., Przekop, A., 2005, "The effect of basis selection on static and random acoustic response prediction using a nonlinear modal simulation," NASA/TP-2005-213943.

[15] Segalman, D., Dohrmann, C., 1996, "A method for calculating the dynamics of rotating flexible structures, part 1: Derivation," *J. Vib. Acoust.*, **118**(3), pp. 313–317.

[16] Segalman, D., Dohrmann, C., Slavin, A., 1996, "A method for calculating the dynamics of rotating flexible structures, part 2: Example calculations," *J. Vib. Acoust.*, **118**(3), pp. 318–322.

[17] Rizzi, S.A., Przekop, A., 2008, "System identification-guided basis selection for reduced-order nonlinear response analysis,", *J. Sound Vib.*, **315**(3), pp. 467–485.

[18] Tartaruga, I., Elliott, A., Hill, T.L., Neild, S.A., Cammarano, A., 2019, "The effect of nonlinear cross-coupling on reduced-order modelling," *Int. J. Non-Linear Mech.*, **116**, pp. 335–350.

[19] Touzé, C., Thomas, O., Chaigne, A., 2004, "Hardening/softening behavior in non-linear oscillations of structural systems using non-linear normal modes," *J. Sound Vib.*, **273**(1–2), pp. 77–101.

[20] Touzé, C., Amabili, M., 2006, "Nonlinear normal modes for damped geometrically nonlinear systems: application to reduced-order modelling of harmonically forced structures," *J. Sound Vib.*, **298**(4), pp. 958–981.

[21] Hollkamp, J.J., Gordon, R.W., 2008, "Reduced-order models for nonlinear response prediction: Implicit condensation and expansion," *J. Sound Vib.*, **318**(4-5), pp. 1139–1153.

[22] Kuether, R.J., Deaner, B.J., Hollkamp, J.J., Allen, M.S., 2015, "Evaluation of geometrically nonlinear reduced-order models with nonlinear normal modes," *AIAA J.*, **53**(11), pp. 3273–3285.

[23] Kerschen, G., Peeters, M., Golinval, J.C., Vakakis, A.F., 2009, "Nonlinear normal modes, part I: A useful framework for the structural dynamicist," *Mech. Syst. Signal Process.*, **23**(1), pp. 170–194.

List of Tables

List of Figures